Brain networks of affective mentalizing revealed by the tear effect

Takahashi, Haruka K.

DOCTOR OF PHILOSOPHY

Department of Physiological Sciences,

School of Life Science,

SOKENDAI (The Graduate University for Advanced Studies)

2015

Table of Contents

1. Summary

Social cognition includes psychological processes by which we can make inferences about other people. Affective mentalizing is defined as the process of inferring others' affective state (i.e., "I understand how you feel"). Previous neuroimaging and lesion studies have identified a distributed set of brain regions that are involved in affective mentalizing. Especially, the medial prefrontal cortex (mPFC), the precuneus/posterior cingulate cortex (PCC), and the temporo-parietal junction (TPJ) are considered the core network for mentalizing. However, the relative contributions of these nodes to affective mentalizing remain poorly understood.

One approach to clarifying the roles of these nodes is to examine which regions are involved in integrating multiple social signals (e.g., facial expressions and bodily gestures). The integration means a process where social signals are combined to infer the most likely affective state. In the field of multisensory research, if signals of two sensory modalities are integrated in a brain region, such region should not only be activated by each sensory modality, but also show a supra-additive effect, indicated by greater activation than the sum of the individual sensory signals. Likewise, I can expect that, if a region is involved in integrating social signals, such region should show a supra-additive effect of these social signals. The goal of this thesis is to investigate

which nodes of the core network of affective mentalizing are involved in the integration of the two social signals: emotional tears and facial expressions. For this purpose, I conducted a functional magnetic resonance imaging (fMRI) experiment wherein brain activity of humans is non-invasively measured.

Sixty-one healthy female subjects participated in the experiment and rated the sadness of observed others during fMRI scanning. I adopted a two-factor within-subjects factorial design, with two levels of facial expressions (sad and neutral) and three levels of tears (faces with tears, with circles and without tears). Thus, the subject observed six different types of faces: those portraying sad facial expressions with tears, with tear-like circles, and without tears; and those portraying neutral facial expressions with tears, with tear-like circles, and without tears. After the standard preprocessing of fMRI data, I utilized the general linear model to estimate brain activity for each type of faces and evaluated the main effects and the interactions within each subject. The supra-additive effect was evaluated as one of the interaction effects. These results from the subjects were summarized to obtain population inferences.

The subjects rated sad facial expressions with tears as sadder than the other types of faces. In the fMRI analysis, the mPFC and PCC showed greater activation when viewing faces with tears than without tears (the main effect of tears), greater

activation when viewing sad face than neutral face (the main effect of facial expressions) and greater activation during the observation of sad facial expressions with tears than the sum of the effects from individual social signals (tears and sad facial expressions) (the supra-additive effect). In contrast to the mPFC and PCC, neither the main effect of sad facial expressions nor the supra-additive effect was found in the TPJ; this region showed only the main effects of tears.

The behavioral results indicate that information on tears and sad facial expressions are combined to infer others' sadness, which is the indicator of the integration. The results of the fMRI analysis indicate that the mPFC and PCC are involved in integrating tears and sad facial expressions. In contrast to the mPFC and PCC, the TPJ was only sensitive to the presence of objects on a face such as tears. These results indicate that the TPJ is engaged in processing tears, but not in the integration of tears and facial expressions.

In conclusion, the mPFC and PCC showed the supra-additive effect of tears and facial expressions in an affective mentalizing task. This result indicates that these midline structures of the cerebral cortex are critical for integrating these social signals, highlighting different roles from the TPJ, the other core node of the mentalizing.

2. Introduction

Social cognition involves psychological processes that allow humans to interact with other individuals in social complex environment (Adolphs, 1999; Frith, 2007). Humans are considered the most social animals among mammals (Adolphs, 1999; Dunbar and Schultz, 2007). Several psychiatric and neurological illnesses are characterized by prominent impairments in social functioning (Kennedy and Adolphs, 2012). Accordingly, there has been considerable interest in the neural mechanisms underlying psychological processes of social cognition (Dunbar and Schultz, 2007; Stanley and Adolphs, 2013).

Among the psychological processes of social cognition, the process of inferring others' affective state is called affective mentalizing (or cognitive empathy) (i.e., "I understand how you feel") (Perry and Shamay-Tsoory, 2013). Previous neuroimaging studies on intact and brain-lesioned patients have shown a widely distributed set of brain regions involved in social cognition (Brothers, 1990; Frith and Frith, 2003; Van Overwalle, 2009; Van Overwalle and Baetens, 2009; Kennedy and Adolphs, 2012). These regions are considered to constitute multiple networks that subserve for distinct processes of social cognition (Van Overwalle and Baetens, 2009; Kennedy and Adolphs, 2012). Among them, the medial prefrontal cortex (mPFC), the precuneus/posterior

cingulate cortex (PCC), and the temporo-parietal junction (TPJ) are considered the core

mentalizing network, because they have often been observed during affective (Atique et

al., 2011; Corradi-Dell'Acqua et al., 2014) and non-affective (cognitive) (Goel et al.,

1995; Van Overwalle, 2009; Van Overwalle and Baetens, 2009) contexts. However, the

relative contributions of these nodes to affective mentalizing are not well understood.

One possible way to clarify the relative contributions of these nodes is to

examine the brain regions that are involved in integrating multiple social signals to infer

others' affective state. Here, I define the integration as a process in which social signals

are combined to infer the most likely affective state. In the field of multisensory

research, if two different types of signal are integrated in a region, it is expected not

only to be activated by each separately (convergence), but also to show interaction

effects between them (Calvert et al., 2000; Raij et al., 2000; Stevenson et al., 2009).

Previous neuroimaging studies have consistently found that the mPFC contains

information about others' emotional state, regardless of whether the social signals

involved facial, body, or vocal expressions (Peelen et al., 2010), or whether they

involved facial expressions or situational information in the absence of observable

expressions (Skerry and Saxe, 2014). These findings indicate that the mPFC plays a key

role in representing others' affective states at the abstract level by receiving information

about distinct social signals. However, each type of social signal was presented separately in previous studies, so it has remained unclear whether the mPFC is involved in the integration process.

Even less is known about the role of the PCC and TPJ in the integration of social signals. In particular, the function of the PCC in mentalizing is not well understood; hence, little attention has been paid to its role in integrating social signals. Furthermore, the function of the TPJ in mentalizing has been controversial (Decety and Lamm, 2007; Mitchell, 2008; Scholz et al., 2009; Cabeza et al., 2012), and its role in the integration of social signals has not been clarified. For instance, Peelen et al. (2010) showed that a region adjacent to the TPJ also contains information about others' emotional state across different types of emotional expressions (face, body, and voice). However, a subsequent neuroimaging study by Skerry and Saxe (2014) utilizing facial expressions and situational information (e.g., social exclusion) showed that the TPJ did not represent others' emotional state at an abstract level; more specifically, their work showed that a classifier, which was trained to discriminate the valence of one social signal within the TPJ, did not successfully classify that valence for the other social signals. Understanding another person's affective state based on situational information is critically different from interpreting emotional expressions (produced by the face,

body, and voice), in that situational information can be interpreted in multiple ways and presents an ill-posed inverse problem (e.g., a person might feel happy *or* sad when he or she is separated from others). Thus, understanding situational information in a socially-appropriate manner requires knowledge of the social event (e.g., that separation from others should be considered a sad event; Barbey et al., 2009; Krueger et al., 2009). Thus, I anticipate that the TPJ plays a minor role in the integration of social signals that involve social event knowledge.

Given this background, I focused my investigation on the integration of two social signals from facial stimuli: tears and facial expressions. To the best of my knowledge, neither the neural mechanisms underlying the processing of tears as social stimuli nor the neural bases of the integration of tears and facial expressions has been identified. Emotional tears appear to be unique to humans and are of considerable interest in the field of evolutionary psychology (e.g., Murube et al., 1999; Provine et al., 2009; Balsters et al., 2013). Like social situations, understanding another's affective state from tears is an ill-posed inverse problem, because tears can be shed in response to many different emotions (e.g., anger, happiness, and sadness; Murube et al., 1999). Therefore, tears are similar to social situations in that they require social event knowledge in order to achieve the most appropriate interpretation. In the absence of

contextual information, humans tend to interpret tears as a symbol of sadness (i.e., the tear effect; Provine et al., 2009), possibly because such an interpretation is the most socially appropriate. As the mPFC can represent others' emotions at an abstract level across different social signals (Peelen et al., 2010; Skerry and Saxe, 2014), I predicted that it would be involved in integrating tears and facial expressions.

The present study used functional magnetic resonance imaging (fMRI) the hypothesis that the mPFC, but not the TPJ, integrates tears and facial expressions during the evaluation of others' sadness. I also explored the role of the PCC in this integration process without a specific hypothesis. I manipulated two factors: tears (tears, tear-like control objects, and no object) and facial expressions (sad and neutral). I initially tested my assumption that the core mentalizing network is activated by the presence of tears, and then examined whether this network shows interaction effects between tears and facial expressions. I predicted that the mPFC would show a supra-additive effect, providing evidence of the integration of information on tears and facial expressions (Meredith and Stein, 1983; Calvert et al., 2000; Raij et al., 2000; Stevenson et al., 2009). In other words, these regions should show stronger activation in response to a sad facial expression with tears than the sum of the activity in response to individual presentations

of a sad facial expression without tears and a neutral facial expression with tears. By

contrast, I predicted that the TPJ would not show the same effect.

3. Materials and methods

3.1. Subjects

Sixty-one healthy subjects aged 18–44 years (mean age = 22.1 years; standard deviation [SD] = 4.7 years) participated in the study. I recruited only female participants because they tend to react to crying people with more sympathy and support than males (Cretser et al., 1982). All subjects were right-handed according to the Edinburgh Handedness Inventory (Oldfield, 1971). None of the volunteers had a history of symptoms requiring neurological, psychological, or other medical care. All subjects gave written informed consent. The study was approved by the ethical committee of the National Institute for Physiological Sciences of Japan. Thirty-eight subjects participated in the main fMRI experiment. The rest of the subjects (n = 23) participated in a separate experiment to define the regions of interest (ROIs). None of the subjects participated in both experiments.

3.2. Data acquisition

fMR images were acquired using a 3T scanner (Verio; Siemens Erlangen, Germany) with a 32-element phased-array head coil. Tight but comfortable foam padding was placed around each subject's head to minimize movement. T2*-weighted

gradient-echo echo-planar imaging (EPI) was used to obtain the functional images. The

sequence parameters were as follows: repetition time (TR), 3,000 ms; echo time (TE),

30 ms; flip angle, 83°; 39 slices of 3.0 mm thickness with a 17% slice gap, which

covered the entire cerebral and cerebellar cortices; field of view, 192 mm; and in-plane

resolution, 3.0×3.0 mm. Oblique scanning was used to exclude the eyeballs from the

images. For anatomical imaging, a T1-weighted three-dimensional (3D)

magnetization-prepared rapid-acquisition gradient echo (MP-RAGE) sequence was

obtained (TR = 1,800 ms; TE = 2.97 ms; flip angle = 9°; field of view = 250 mm; and

voxel dimensions = $0.9 \times 0.9 \times 1.0$ mm).

3.3. Stimuli

I used six types of faces: those portraying sad facial expressions with tears,

with tear-like circles, and without tears; and those portraying neutral facial expressions

with tears, with tear-like circles, and without tears (**Figure 1A**). Stimuli were produced

as described below.

3.3.1. Stimuli production

I followed the same procedure as Provine et al. (2009) to produce the stimuli. I initially obtained 90 images of faces with tears (Tears images) from the online image archives Flickr (www.flickr.com) and Google (www.google.co.jp). I limited my search to images of female adults in order to eliminate gender differences between the subjects and stimuli. In addition to facial images, I also collected 45 landscape images from Flickr to use as controls.

I removed the tears from the 90 face images using photo-editing software (Adobe Photoshop, Adobe Systems Inc., San Jose, CA) and defined them as NoTears images. I then produced new images by adding gray circles to the NoTears images, resulting in the Circles images. The location and the number of gray circles in the Circles images were matched with the location and number of tears in the original (Tears) images. I did not include natural objects on stimuli (e.g., scars or saliva) in order to match the locations of stimuli and to avoid any possible interpretation of affective states (e.g., the observed person is hungry because of saliva on the face). Collectively, I created three sets of facial images (comprising 270 images in total): 90 Tears images, 90 NoTears images, and 90 Circles images. The mean differences in size and perceived brightness of the images for each condition were minimized using photo-editing software (Adobe Photoshop, Adobe Systems Inc., San Jose, CA).

I further categorized each set of images into two subsets (sad and neutral)

based on their facial expressions. Eight females, who did not participate in the fMRI

experiment, rated the intensity of sadness in the images on a visual analogue scale

(VAS) ranging from 0 ("not sad at all") to 100 ("extremely sad"). Initially, I used the

VAS scores from the same eight subjects to classify the 90 NoTears images into 45

images of "sad" expressions and 45 images of "neutral" expressions. Then, the Tears

and Circles images were categorized into "sad" and "neutral" images; the images for

each facial expression were identical except for the presence of tears or circles. In total,

I produced seven types of image: sad facial expressions with tears (Sad Expression +

Tears [ST] images), sad facial expressions without tears (Sad Expression [S] images),

sad facial expressions with circles (Sad Expression + Circles [SC] images), neutral

facial expressions with tears (Neutral + Tears [NT] images), neutral faces without tears

(Neutral [N] images), neutral faces with circles (Neutral + Circles [NC] images), and

landscape images (Baseline [B] images) (**Figure 1A**). **Figure 1** shows schematic

drawings of representative stimuli due to copyright issues. Each image was used only

once in each experiment.

3.3.2. Stimulus presentation

Stimuli were back-projected via a liquid crystal display (LCD) projector

(CP-SX12000; Hitachi, Ltd., Tokyo) onto a translucent screen located at the rear of the

scanner. The horizontal and vertical viewing angles of stimuli were 5.3 and 7.4°,

respectively. The subjects viewed stimuli via a mirror placed above the head coil. I used

Presentation software to display visual stimuli and record the subject's response

(Neurobehavioral Systems, Inc., San Francisco, CA).

3.4. Task design and procedure

A two-factor within-subjects factorial design was used, with two levels of

Facial Expressions (Sad and Neutral) and three levels of Tears (Tears, NoTears and

Circles) (**Figure 1A**). In addition to these six conditions, I included a baseline (B)

condition, during which subjects observed landscape images.

I employed a conventional block design (**Figure 1B**) with five runs. Each run

consisted of the first 12 scan volumes, followed by 23 blocks that lasted for 18 s (6

volumes per block), and the final 6 volumes (12 volumes + [23 blocks × 6 volumes] + 6

volumes = 156 volumes per run). Each block included one of the seven task conditions,

and each condition was repeated three times (21 blocks). Each block included three

trials of the same condition, and each trial lasted 6 s (3 blocks × 3 trials per block × 5

runs = 45 trials for each condition in total). The order of the conditions was

pseudo-randomized in each repetition. In addition, I included two blocks of the rest

condition: one between the last block of the first repetition of a condition and the first

block of the second repetition; and the other between the last block of the second

repetition and the first block of the third repetition (2 rest blocks + 21 task blocks = 23

blocks in total).

In each trial, an image was presented for 3.5 s, followed by the presentation of

a visual analog scale (VAS) for 2.5 s. The subjects used the VAS to evaluate the extent

of sadness of the presented facial stimuli. The subjects manipulated a two-button

response box (HHSC-2x2, Current Designs, Inc., Philadelphia, PA) with their right

hand to specify the location of the vertical line on a VAS (the index finger moved the

line to the left, and the middle finger moved the line to the right). The VAS scale

consisted of a white-colored horizontal bar with each end indicating the minimum (i.e.,

not sad at all) and the maximum (i.e., extremely sad) of the intensity of sadness

expressed by the image. The vertical line on the VAS was always located at the center

of the horizontal bar at the onset of rating phase (i.e., 3.5 s after the onset of the trial).

The end of the minimum and maximum was counterbalanced across the subjects. In the

baseline (B) condition, the subject was asked to move the VAS to any position they

wished. All of the subjects performed several practice trials in order to familiarize them

with the task and to ensure they were able to utilize the VAS easily.

3.5. Imaging data processing

The first six volumes of each fMRI run were discarded for stabilization of the

magnetization, and the remaining 150 volumes per run (a total of 750 volumes per

participant) were used for analysis. Image processing and statistical analyses were

performed using the Statistical Parametric Mapping (SPM8) package (Friston et al.,

2007). The images were realigned to correct for head motion, then corrected for

differences in slice timing within each volume. After the T1-weighted anatomical

images were segmented into different tissue classes, each subject's T1-weighted

anatomical image was co-registered with the mean image of all of the EPI images for

each subject. Each co-registered T1-weighted anatomical image was normalized to the

Montreal Neurological Institute T1 image template (ICBM 152) (Evans et al., 1994;

Friston et al., 1995). The parameters from this normalization process were then applied

to each functional image. The spatially normalized EPI images were filtered using a

Gaussian kernel of 8 mm full width at half maximum (FWHM) in the x, y, and z axes

(final smoothness: x = 11.8, y = 11.9, and z = 11.8 mm). The parameters from this

normalization process were then applied to the functional images, which were

resampled to a final resolution of $2 \times 2 \times 2$ mm^3.

3.6. Statistical analyses

3.6.1. Individual analyses

A design matrix comprising the five runs was prepared for each subject. I fitted

a general linear model (GLM) to the fMRI data for each subject (Friston et al., 1994a;

Worsley and Friston, 1995). Neural activity during each condition was modeled with

box-car functions convolved with the canonical hemodynamic-response function. Each

run included seven task-related regressors, one for each condition. The time series for

each voxel was high-pass filtered at 1/128 Hz. Assuming a first-order autoregressive

model, the serial autocorrelation was estimated from the pooled active voxels with the

restricted maximum likelihood (ReML) procedure, and was used to whiten the data

(Friston et al., 2002). Motion-related artifacts were minimized by incorporating six

parameters (three displacements and three rotations) from the rigid-body realignment

stage into each model. The parameter estimates for each condition in each individual

were compared using linear contrasts. After confirming face-related activation (e.g.,

activation in the fusiform gyrus) by comparing face conditions with baseline (B), I

evaluated the following contrasts (**Table 1**): first, Tears minus NoTears, [(ST + NT) −

(S + N)]; second, Circles minus NoTears, [(SC + NC) − (S + N)]; third, Tears minus

Circles, [(ST + NT) − (SC + NC)]; fourth, Sad minus Neutral expressions, [(ST + S +

SC) − (NT + N + NC)]; and fifth, interaction effects, [(ST − SC) − (NT − NC)] and [(NT

− NC) − (ST − SC)]. The supra-additive effect was tested by the contrast of [(ST − SC) −

(NT − NC)] (i.e., (ST − NC) > (SC − NC) + (NT − NC)).

3.6.2. Random-effects group analysis

In the individual analysis, I obtained images that represent the normalized

task-related increment of the MR signal of each subject for each predefined contrast (i.e.,

contrast images). These contrast images were used for the group analysis. For each

predefined contrast (**Table 1**), a one-sample t-test was performed for every voxel in the

brain to obtain population inferences (Holmes and Friston, 1998). The resulting set of

voxel values for each comparison constituted an SPM of the t statistic SPM {t}. The

height threshold for the SPM {t} was set at t (37) > 2.72, equivalent to p < 0.005

uncorrected. The statistical threshold for the spatial extent test on the clusters was set at

p < 0.05 and corrected for multiple comparisons (family-wise error [FWE]) over the

whole brain (Friston et al., 1994b; 1996).

Brain regions were anatomically defined and labeled according to probabilistic atlases (Amunts et al., 2005; Eickhoff et al., 2005; Shattuck et al., 2008) and a previous meta-analysis study (Van Overwalle, 2009). In order to avoid the ambiguity of the anatomical location of the TPJ, I defined it as the angular gyrus (Saxe and Powell, 2006; Scholz et al., 2009; Cabeza et al., 2012). Consistent with a meta-analysis (Van Overwalle, 2009), I defined the mPFC as the medial wall of the prefrontal cortex: that is, regions in which the x coordinates ranged from -20 to 20 and the y coordinates were above $y > 20$ in MNI space (Van Overwalle, 2009). I further subdivided the mPFC into three regions (Van Overwalle, 2009): the dorsomedial prefrontal cortex (dmPFC), which lies above the z coordinate of 20 mm; the ventromedial prefrontal cortex (vmPFC), which lies between $z = -15$ and $z = 20$ mm; and the medial orbitofrontal cortex (mOFC), which lies below $z = -15$ mm.

3.6.3. ROI analysis

After the whole-brain analysis was completed, ROI analysis was conducted in order to further examine activation patterns in mPFC, PCC and TPJ. The supra-additive effect of the two distinct signals would be observed in brain regions which are activated by each signal. Accordingly, I assumed that the supra-additive effect should be observed

within the regions that were more active during the Tears condition than the NoTears

condition, which is a more liberal control than the Circles conditions (SC and NC). I

defined ROIs based on the brain regions that were activated by the Tears condition

relative to the NoTears condition.

The use of the same dataset for the definition of ROI and analysis of response

patterns in the ROI can lead to invalid statistical inferences (i.e., the double-dipping

problem; Kriegeskorte et al., 2009). To avoid this, I conducted a separate experiment to

compare the Tears condition with the NoTears condition, as described below.

3.6.3.1. Task design and analyses for a separate experiment. The design and analyses

of this experiment were identical to the main experiment except that the Circles

conditions (SC and NC) were removed (3 blocks for each condition $\times$ 5 conditions + 2

rest blocks = 17 blocks). I collected 9 volumes before the first block and 7 volumes after

the last block (9 + [17 blocks $\times$ 6] + 7 = 118 volumes per run). The threshold for the

SPM {t} was set at t (22) > 2.82 (equivalent to $p < 0.005$ uncorrected, which was the

same height threshold as that in the main experiment). The statistical threshold for the

spatial extent test on the clusters was set at $p < 0.05$ and corrected for multiple

comparisons (FWE) over the whole brain (Friston et al., 1994b; 1996).

I evaluated only the Tears vs. NoTears contrast [(ST + NT) − (S + N)]. I chose

the peak coordinates in each cluster in the mPFC, PCC, and TPJ. A cluster of activation

could include anatomical regions beyond my hypothesis (e.g., the fusiform gyrus in the

TPJ ROI). In order to limit the ROIs to each hypothesized region, I calculated the

overlap between the cluster activated by the tear effect and a 12-mm-radius sphere with

the peak coordinates of the same cluster. This radius was identical to the effective

resolution (final smoothness) of the statistical parametric maps. This overlapping region

in each cluster was used as the ROI.

Using these ROIs, I conducted two different types of analysis on the data from

the main experiment: univariate and multi-voxel pattern analyses (MVPA). For both, I

used unsmoothed data in order to maximize sensitivity, and to allow for the extraction

of the full information present in the spatial patterns of the fMRI data, which could have

been reduced by the smoothing (Haynes et al., 2007).

3.6.3.2. Univariate analyses. I averaged the contrast estimates in all voxels within each

ROI. I conducted the analyses on the contrast estimates of the four conditions of interest

(ST, SC, NT, and NC).

3.6.3.3. Multi-voxel pattern analyses (MVPA). The role of the TPJ in mentalizing has

been controversial (Decety and Lamm, 2007; Mitchell, 2008; Scholz et al., 2009;

Cabeza et al., 2012). More specifically, while the TPJ is activated by both mentalizing

and attention reorienting (Mitchell, 2008), the detailed spatial patterns between these

conditions can differ (Scholz et al., 2009). In order to clarify the function of the TPJ, I

conducted the MVPA (Haxby et al., 2001; Peelen et al., 2006). The MVPA was

complementary to the univariate analysis in that it was sensitive to differences in spatial

patterns of activation between the conditions, even though they showed a similar height

of activation in the univariate group analysis.

I calculated voxel-wise within-factor correlations (i.e., between independent

runs of the Tears conditions and between independent runs of the Circles conditions)

and between-factor correlations (i.e., between the Tears and Circles conditions) in each

ROI for each subject. Within-factor runs indicate the consistency of activation patterns

across runs, whereas between-factor runs indicate the spatial relationship between the

Tears and Circles conditions. Therefore, greater correlation coefficients in the

within-factor of Tears relative to the between-factor correlations indicate that Tears and

Circles show different patterns of activation. I detail these analyses below.

I initially prepared two design matrices for each subject, one including the first and third (odd-numbered) runs and the other including the second and fourth (even-numbered) runs. I excluded the fifth run from the analysis in order to equate the number of runs between the two design matrices. In each design matrix, I evaluated the contrasts of [(ST + NT) − (S + N)] (the Tears contrast) and [(SC + NC) − (S + N)] (the Circles contrast). The t values of each voxel in the ROIs were extracted from each SPM {t} image for all subjects. Then, in order to calculate the within-factor correlations, I computed the correlation coefficients of the SPM {t} between the even runs and the odd runs for the Tears contrast, and between the even runs and odd runs for the Circles contrast. Likewise, I calculated the between-factor correlation coefficients between the even runs of the Tears contrast and the odd runs of the Circles contrast, and between the odd runs of the Tears contrast and the even runs of the Circles contrast. These coefficients were transformed into Z values, which conform to a normal distribution.

4. Results

4.1. Behavioral results

The presence of tears on the face images increased the VAS ratings of sadness (**Figure 2**). A two-way repeated-measures analysis of variance (ANOVA) (2 levels of Facial Expressions × 3 levels of Tears) on the rating scores revealed significant main effects of Facial Expressions [$F(1, 37) = 635.8$, $p < 0.001$] and of Tears [$F(2, 74) = 142.5$, $p < 0.001$], and a significant interaction [$F(2, 74) = 94.2$, $p < 0.001$]. Post-hoc pair-wise comparisons (with a Bonferroni correction) showed that there were greater VAS ratings in the Tears condition compared with the NoTears and Circles conditions for each facial expression (p values < 0.001). The effect of tears on the VAS ratings was greater for the neutral expressions than for the sad expressions, regardless of whether the Tears condition was compared to the NoTears or Circles conditions (p values < 0.001). Finally, I found that the Circles condition showed greater VAS rating scores than the NoTears condition for neutral expressions ($p < 0.01$), but not for sad facial expressions ($p > 0.9$).

Taken together, these findings confirm that the presence of tears increased the sadness ratings (Provine et al., 2009).

4.2. fMRI results

4.2.1. Whole-brain analysis

4.2.1.1. The main effect of tears. I conducted the three contrasts to evaluate activity of

the brain regions by the presence of tears and circles: that is, the contrast of Tears with

NoTears, the contrast of Circles with NoTears and the contrast of Tears with Circles.

NoTears and Circles were considered liberal and stringent controls, respectively. The

contrast of Tears minus NoTears [(ST + NT) − (S + N)] revealed regions of significant

activation bilaterally in the vmPFC, mOFC, posterior cingulate gyrus, TPJ, superior

parietal lobule, superior, middle and inferior occipital gyri, middle and inferior temporal

gyri, fusiform gyrus, and caudate nucleus (**Figure 3 and Table 2**). In addition, the same

contrast revealed significant activation in the left hemisphere: specifically, in the

dmPFC, precuneus, middle frontal gyrus, superior temporal gyrus, amygdala,

hippocampus and brainstem.

The contrast of Circles minus NoTears [(SC + NC) − (S + N)] revealed regions

of significant activation bilaterally in the TPJ, precuneus, superior parietal lobule,

superior, middle and inferior occipital gyri, supramarginal gyrus, middle and inferior

temporal gyri, fusiform gyrus, parahippocampal gyrus and cerebellum (**Figure 4 and**

Table 3). In addition, the same contrast revealed significant activation in the left

28

hemisphere: specifically, in the precentral gyrus, postcentral gyrus, middle and inferior frontal gyrus.

The contrast of Tears minus Circles [(ST + NT) − (SC + NC)] revealed no significant activation.

4.2.1.2. The main effect of sad expressions. The contrast of Sad minus Neutral expressions [(ST + SC + S) − (NT + NC + N)] revealed significant activation bilaterally in the mPFC (dmPFC, vmPFC, and mOFC), precuneus, and posterior cingulate gyrus (**Figure 5 and Table 4**). In addition to these regions, the same contrast revealed bilateral activation in the precentral gyrus, postcentral gyrus, superior frontal gyrus, superior parietal lobule, cuneus, caudate nucleus, insula, putamen, superior and middle temporal gyri, parahippocampal gyrus, hippocampus, amygdala, and fusiform gyrus. I also found activation in the left cerebellum, left inferior temporal gyrus, right supramarginal gyrus, and right lingual gyrus.

4.2.1.3. Interactions between Tears and Sad facial expressions. The contrast of the supra-additive effect [(ST − SC) − (NT − NC)] revealed bilateral activation in vmPFC, posterior cingulate gyrus, precuneus, cuneus, parahippocampal gyrus, lingual gyrus,

cerebellum, amygdala, and hippocampus. Moreover, the same contrast revealed

significant activation in the left dmPFC and right mOFC (**Figure 6 and Table 5**). The

opposite contrast [(NT − NC) − (ST − SC)] revealed no significant activation.

Collectively, activity in the mPFC and PCC showed the main effect of tears,

the main effect of sad expressions, and the supra-additive effect. By contrast, activity in

the TPJ showed only effects related to tears and circles. In order to further characterize

response patterns in these regions, I conducted the following ROI analysis.

4.2.2. ROI analysis

4.2.2.1. ROI definitions. In the whole-brain analysis, only the main effect of tears

showed activation in all nodes of the core mentalizing network (the mPFC, PCC, and

TPJ). Thus, I functionally defined ROIs based on this effect. In order to avoid the

double-dipping problem (Kriegeskorte et al., 2009), I conducted a separate fMRI

experiment to localize the mPFC, PCC, and TPJ. I found six clusters of significant

activation (**Figure 7 and Table 6**). Among these, the following five clusters

corresponded to the core mentalizing network: one cluster in the superior mPFC

(dmPFC and vmPFC); one cluster in the inferior mPFC (mOFC and vmPFC); one

cluster in the PCC; one cluster in the left TPJ; and one cluster in the right TPJ. I used

these five ROIs in the analyses (**Figure 8A**).

4.2.2.2. Univariate analysis. **Figure 8B** shows the contrast estimates (i.e., the activity

relative to the Neutral NoTears [N] condition) for the four conditions of interest. I

confirmed that the contrast estimates in the ST, SC, and NT conditions were

significantly greater than the N condition in all ROIs except for the SC condition in the

superior mPFC (p values < 0.05, one-tailed one-sample t tests). More specifically, the

same statistical test showed a tendency toward significance in the SC condition of the

superior mPFC ($t(37) = 1.6$, $p = 0.06$).

The PCC and two clusters in the mPFC showed greater activity in the ST

condition compared to the other three conditions. Two-way ANOVAs (2 levels of Tears

$\times$ 2 levels of Facial Expressions) on the contrast estimates of these regions showed

significant main effects of Tears [$F(1, 37) = 8.9$, $p < 0.01$ for the PCC; $F(1, 37) = 8.7$, p

< 0.01 for the inferior mPFC; and $F(1, 37) = 10.3$, $p < 0.01$ for the superior mPFC] and

Facial Expressions [$F(1, 37) = 13.9$, $p < 0.01$ for the PCC; $F(1,37) = 23.9$, $p < 0.001$ for

the inferior mPFC; and $F(1, 37) = 8.6$, $p < 0.01$ for the superior mPFC]. The same

ANOVA also revealed significant interactions between the two factors in the PCC [$F(1,$

31

37) =10.4, p < 0.01] and inferior mPFC [F(1, 37) =6.2, p < 0.05], and an interaction

showing a trend toward significance in the superior mPFC [F(1, 37) = 3.7, p = 0.06].

Post-hoc pairwise comparisons (with a Bonferroni correction) in these regions showed

significantly greater contrast estimates in the ST than the SC condition (p values < 0.01),

whereas there were no such differences between the NT and NC conditions (p values >

0.2).

In contrast to the midline regions, I observed no such differences in the TPJ.

The same two-way ANOVAs (2 levels of Tears × 2 levels of Facial Expressions)

revealed neither significant main effects (p values > 0.06) nor interactions (p values >

0.3).

4.2.2.3. Multi-voxel pattern analysis (MVPA). As shown above, in the TPJ, I found

neither an effect of Tears (i.e., greater activity in Tears relative to Circles conditions)

nor an interaction with facial expressions. Given the recent controversy about the role of

the TPJ (Decety and Lamm, 2007; Mitchell, 2008; Scholz et al., 2009; Cabeza et al.,

2012), it is possible that activation in the TPJ merely reflects the detection of small

objects on the face (i.e., tears and circles) (Decety and Lamm, 2007; Mitchell, 2008).

Alternatively, neural populations that subserve different functions (mentalizing and

attention reorienting) might be located in neighboring but distinct regions within the

TPJ (Scholz et al., 2009). In order to address this point, I conducted an MVPA analysis

in each ROI to compare activation patterns between the Tears and Circles conditions.

Figure 9 shows the plot of the correlation coefficients in each ROI. One-way

ANOVAs (Tears, Circles, and Tears vs. Circles) on the Z scores of the correlation

coefficients for each ROI revealed a significant main effect in the bilateral TPJ and

superior mPFC [$F_{(2, 74)} = 3.2$, $p < 0.05$ for the left TPJ; $F_{(2, 74)} = 3.8$, $p < 0.05$ for

the right TPJ; and $F_{(2, 74)} = 3.7$, $p < 0.05$ for the superior mPFC]. Neither the inferior

mPFC nor the PCC showed a significant main effect (p values > 0.05). Post-hoc

pair-wise comparisons (with the Bonferroni correction) revealed that the within-factor

of Tears showed greater correlation coefficients than the between-factor of Tears and

Circles in the bilateral TPJ and superior mPFC (p values < 0.05). No other significant

differences were observed (p values > 0.1).

5. Discussion

In the present study, the mPFC and PCC showed a supra-additive effect between sad facial expressions and the presence of tears. In contrast, the TPJ only showed different patterns of activation between tears and circles, revealed by the MVPA.

5.1. Behavioral performance

I confirmed the tear effect (Provine et al., 2009) by showing that the observation of tears increased ratings of sadness compared with control conditions in which there were no tears (no tears and circles conditions; **Figure 2**). I also found interaction effects between sad facial expressions and tears: the tear effect was smaller for sad expressions than for neutral expressions. In other words, a signal of sadness shows a reduced effect when another indicator of sadness is already present. This sub-additive effect might be explained by Weber's law, which states that the change in stimulus intensity that can be discriminated is a constant fraction of the intensity of the original stimulus (e.g., facial expressions, Gao et al., 2013).

5.2. Tear effect in the mPFC, PCC, and TPJ

I found that all nodes of the core mentalizing network (mPFC, PCC, and TPJ) were activated when rating the sadness of faces with tears compared to faces without tears (**Figures 3 and 8B**). To the best of my knowledge, only one study has examined the brain activity of the tear effect. More specifically, Hendriks et al. (2007) examined an early event-related potential (ERP) component (N170) in response to faces when the subject observed crying (with tears) and other facial expressions. However, neither the latency nor the amplitude of the ERPs differed between crying and other facial expressions. To the best of my knowledge, the present study is the first that has identified the neural substrates underlying the tear effect.

5.3. Supra-additive effect between tears and facial expressions in the mPFC and PCC

I found that the inferior mPFC (covering the mOFC and vmPFC) and the PCC showed not only main effects of facial expressions and tears, but also the supra-additive effect between them. As in the field of multisensory research, my result indicates that the mPFC and PCC are involved in integrating tears and facial expressions for the purpose of inferring others' sadness. In other words, these regions might be engaged in combining the perceived social signals to infer the most likely extent of others' sadness.

Previous lesion studies showed that damage to the orbitofrontal cortex (OFC), a part of the mPFC, produces impairments in the recognition of social signals involving emotional facial expressions (Hornak et al., 1996; Blair and Cipolotti, 2000; Rolls, 2004; Dal Monte et al., 2013; Willis et al., 2014) and emotional vocal expressions (Hornak et al., 1996; Hornak et al., 2003; Rolls, 2004). In accord with these findings, previous neuroimaging studies have indicated that the mPFC contains abstract representations of others' emotional states regardless of the type of social signal (Peelen et al., 2010; Skerry and Saxe, 2014). However, as each type of social signal was presented separately in these studies, it was unclear whether the mPFC showed an interaction effect between multiple social signals. Moreover, unlike the mPFC, the role of the PCC has been poorly investigated in the context of mentalizing. The current study revealed that the mPFC and PCC showed an interaction effect between distinct social signals during affective mentalizing, providing more direct evidence for the integration of social signals in these regions.

One explanation of this result is that the integration process is conducted in other brain regions, and the supra-additive effect in the mPFC and PCC represents the extent of others' sadness provided by such an integration process. However, this interpretation was not supported by the following two findings. First, only the mPFC

and PCC consistently met the criteria of convergence (i.e., were activated by each social signal) and interaction. Second, if the supra-additive effect in the mPFC represents the degree of sadness, the supra-additive effect should be also observed in the behavioral result. However, the sub-additive effect, but not the supra-additive effect, was observed in the sadness rating (**Figures 2 and 8B**). Thus, it is unlikely that the supra-additive effect simply represents the extent of sadness. Rather, the supra-additive effect is better explained by the hypothesis that integrating two different social signals (for the purpose of affective mentalizing) imposes greater processing demands in the mPFC and PCC than individual signals.

The core mentalizing network (such as the mPFC and PCC) and the human homologue of the mirror-neuron system (e.g., the inferior frontal gyrus and inferior parietal lobule) are both active during the recognition of others' facial emotions (Phan et al., 2002; Carr et al., 2003; Winston et al., 2003; Lennox et al., 2004; Vytal and Hamann, 2010; Kitada et al., 2013). As compared to the mirror-neuron system, the core mentalizing network seems to be active when observers reflect on the cause of the behavior — e.g., why is this person shedding tears? (Van Overalle and Beatens, 2009). The core mentalizing network is also proposed to be a part of the social "reflective system" (C system), a slow system that is responsible for taking situational constraint

information and other prior knowledge into account for mentalizing (Satpute and

Liberman, 2006). In order to determine that the person shedding tears is sad, we rely on

knowledge based on previous experience. Consistent with this view, the PCC is

associated with long-term memory (Minoshima et al., 1997; Ranganath et al., 2004;

Wagner et al., 2005; Cavanna and Trimble, 2006; Matsuda, 2007). For instance,

Alzheimer's disease (AD) is characterized not only by medial temporal lobe (MTL)

atrophy, but also by a reduction of glucose metabolism in the cingulo-parietal cortex,

including the precuneus (Matsuda, 2007). Activity in the precuneus is reduced in

patients with very-early-stage AD who exhibit only memory impairment, without

general cognitive decline (Minoshima et al., 1997). The default mode network (DMN),

including the mPFC and PCC, is often associated with mind wandering, which can

result in the retrieval of an episodic memory (Mason et al., 2007; Spreng et al., 2009).

In the present study, the PCC showed activation not only in the presence of tears, but

also during the observation of sad facial expressions (relative to neutral expressions;

Figures 5 and 8B). Therefore, the PCC might be involved in the retrieval of the social

meaning of tears (i.e., as a symbol of sadness) from long-term memory, and the

integration of the retrieved social knowledge with the sad facial expressions.

In addition to the PCC, I found the supra-additive effect in the inferior mPFC, including the mOFC and vmPFC. Subregions in the mPFC are thought to play distinct but complementary roles in mentalizing (Amodio and Frith, 2006; Krueger et al., 2009). Krueger et al. (2009) proposed that the inferior mPFC supports inferences about the likely affective response and reward value accompanying goal achievement. According to this hypothesis, the process of integrating tears and facial expressions in this region might reflect the evaluation of the state of sadness (i.e., how sad is this person?). Lesions in the OFC can lead to abnormal social judgments in response to emotional faces (Willis et al., 2010). More specifically, the subjects in this study were presented with faces portraying emotional expressions and asked to imagine whether they would approach them to ask for directions. Compared to control (intact) subjects and patients with damage to frontal regions sparing the OFC, the patients with damage to the OFC tended to have abnormal approachability judgments: OFC patients rated faces displaying negative emotional expressions as significantly more approachable than the other subject groups.

I also found that the superior mPFC showed a tendency toward the supra-additive effect (**Figure 8B**). The MVPA showed that, unlike the inferior mPFC and PCC, the superior mPFC showed different patterns of activation between tears and

circles (**Figure 7**). This result indicates different roles between the superior and inferior mPFC. The superior mPFC is thought to support inferences about the likely actions performed by others for goal achievement (i.e., why is this person shedding tears?) (Krueger et al., 2009). As such, it is possible that, along with the PCC, these subregions in the mPFC might work in concert to infer others' state of sadness at an abstract level.

I also observed the supra-additive effect in areas of the limbic system such as the MTL and amygdala (**Table 5**). The supra-additive effect in the MTL is consistent with my speculation that the social knowledge of tears is retrieved from long-term memory and integrated with sad facial expressions (Eldridge et al., 2000; Miyashita, 2004). The amygdala is considered as a part of the social "reflexive system" (X system), which automatically and quickly evaluates others' behavior (Satpute and Lieberman, 2006). Thus, this reflexive system (X system) might be engaged in the integration of social signals directly (Morris et al., 1998) or indirectly via the top-down modulation from parts of the reflective system (C system), such as the mPFC and PCC (Ochsner et al., 2002; Pessoa et al., 2002). However, unlike the mPFC and PCC, the MTL and amygdala were not consistently activated by the presence of tears in the two experiments; they were not activated in the separate experiment (**Figure 7 and Table 6**).

Therefore, further studies are necessary to examine whether the MTL and amygdala are important for the integration of tears and facial expressions.

5.4. No interaction effect in the TPJ

Like the mPFC and PCC, the TPJ showed greater activation when viewing faces with tears than without tears, which was a more liberal control than circles (**Figures 3 and 8A**). However, the TPJ differed from the mPFC and PCC in two ways: first, I observed no interaction between facial expressions and tears (**Figure 8B**); and second, although the TPJ was also activated by control circles (relative to faces without tears), detailed spatial patterns of activation differed between tears and control circles (**Figure 9**). These results indicate that the TPJ is engaged not in the integration of signals related to tears and facial expressions, but rather in the processing of objects on a face like tears.

The TPJ is thought to be a hub of diverse functions, including perceptual/motor reorienting and theory of mind (Cabeza et al., 2012). In the present study, I minimized differences in the locations and sizes of the tears and circles. Thus, it is unlikely that different activation patterns within the TPJ are due to different degrees of attention orienting between tears and tear-like circles. Scholz et al. (2009) showed neighboring

but distinct patterns of activation in the TPJ between mentalizing (i.e., false-belief story) and spatial attention tasks (Posner paradigm; Corbetta and Shulman, 2002). Therefore, it is reasonable to interpret the different activation patterns in the TPJ between tears and circles as reflecting different processing between the two stimuli.

It has been proposed that one of the general functions of the TPJ is to detect a mismatch between our expectations and actual outcomes (Corbetta et al., 2008; Koster-Hale and Saxe, 2013). More specifically, the TPJ is activated when a target is presented in an unexpected location in spatial attention tasks (Posner paradigm; Corbetta and Shulman, 2002). False-belief stories, which are often used in mentalizing tasks, require processing information detected outside the main focus of attention (Cabeza et al., 2012). Shedding tears (in adults) and circles are rarely observed in our daily life, whereas the activation pattern between tears and circles differed in the TPJ. Therefore, it is possible that the TPJ is involved in detecting and perceiving unusual objects such as tears.

5.5. Limitations

Three limitations must be considered. First, I utilized pictures of different individuals between the sad and neutral conditions. It is unlikely that the supra-additive

effect is also affected by the difference in facial identity, because this factor is

subtracted out in the supra-additive effect [(ST – SC) – (NT – NC)]. However, I cannot

rule out the possibility that greater activation in sad expressions (relative to neutral

expressions) can be partially explained by different facial identity. Second, female

subjects only participated in present study, because they tend to react to crying people

with more sympathy and support than males (Cretser et al., 1982). However, future

studies should test whether this finding can be generalized to male subjects, and

examine the integration of facial expressions and tears in genders that are different from

the subjects (the cross-gender effect). Finally, I used the sad and neutral facial

expressions. However, tears can be shed in response to many different emotions

(Murube et al., 1999). Future studies should test whether the same supra-additive effect

can be observed when others facial expressions were integrated with tears in affective

mentalizing.

6. Conclusions

The present study investigated which nodes of the core mentalizing network are involved in the integration of tears and facial expressions that are used to infer the extent of others' sadness. I found that the mPFC and PCC showed a supra-additive effect between tears and facial expressions. In contrast, the TPJ showed no such effect. These results indicate that the mPFC and PCC are involved in integrating distinct social signals to represent others' sadness at an abstract level. These results highlight the differences in the contributions of the mPFC, PCC, and TPJ to affective mentalizing.

7. Acknowledgments

8. References

Adolphs, R,. 1999. Social cognition and the human brain. Trends. Cogn. Sci. 3, 469–479.

Amodio, D.M., Frith, C.D., 2006. Meeting of minds: the medial frontal cortex and social cognition. Nat. Rev. Neurosci. 7, 268–277.

Amunts, K., Kedo, O., Kindler, M., Pieperhoff, P., Mohlberg, H., Shah, N.J., Habel, U., Schneider, F., Zilles, K., 2005. Cytoarchitectonic mapping of the human amygdala, hippocampal region and entorhinal cortex: intersubject variability and probability maps. Anat. Embryol. (Berl.) 210, 343–352.

Atique, B., Erb, M., Gharabaghi, A., Grodd, W., Anders, S., 2011. Task-specific activity and connectivity within the mentalizing network during emotion and intention mentalizing. Neuroimage 55, 1899–1911.

Balsters, M.J.H., Krahmer, E.J., Swerts, M.G.J., Vingerhoets, A.J.J.M., 2013. Emotional tears facilitate the recognition of sadness and the perceived need for social support. Evol. Psychol. 11, 148–158.

Barbey, A.K., Krueger, F., Grafman, J., 2009. Structured event complexes in the medial prefrontal cortex support counterfactual representations for future planning. Philos. Trans. R. Soc. Lond. B Biol. Sci. 364, 1291–1300.

Blair, R.J.R., Cipolotti, L., 2000. Impaired social response reversal: A case of 'acquired

    sociopathy'. Brain 123, 1122–1141.

Brothers. L., 1990. The social brain: A project for integrating primate behavior and

    neurophysiology in a new domain. Concepts Neurosci. 1, 27–251.

Cabeza, R., Ciaramelli, E., Moscovitch, M., 2012. Cognitive contributions of the ventral

    parietal cortex: an integrative theoretical account. Trends Cogn. Sci. 16,

    338–352.

Calvert, G.A., Campbell, R., Brammer, M.J., 2000. Evidence from functional magnetic

    resonance imaging of crossmodal binding in the human heteromodal cortex.

    Curr. Biol. 10, 649–657.

Carr, L., Iacoboni, M., Dubeau, M.C., Mazziotta, J.C., Lenzi, G.L., 2003. Neural

    mechanisms of empathy in humans: a relay from neural systems for imitation

    to limbic areas. Proc. Natl. Acad. Sci. USA. 100, 5497–5502.

Cavanna, A.E., Trimble, M.R., 2006. The precuneus: a review of its functional anatomy

    and behavioural correlates. Brain 129, 564–583.

Corbetta, M., Shulman, G.L., 2002. Control of goal-directed and stimulus-driven

    attention in the brain. Nat. Rev. Neurosci. 3, 201–215.

Corbetta, M., Patel, G., Shulman, G.L., 2008. The reorienting system of the human

brain: from environment to theory of mind. Neuron 58, 306–324.

Corradi-Dell'Acqua, C., Hofstetter, C., Vuilleumier, P., 2014. Cognitive and affective

theory of mind share the same local patterns of activity in posterior temporal

but not medial prefrontal cortex. Soc. Cogn. Affect. Neurosci. 9, 1175–1184.

Cretser, G.A., Lombardo, W.K., Lombardo, B., Mathis, S., 1982. Reactions to men and

women who cry: a study of sex differences in perceived societal attitudes

versus personal attitudes. Percept. Mot. Skills 55, 479–486.

Dal Monte, O., Krueger, F., Solomon, J.M., Schintu, S., Knutson, K.M., Strenziok, M.,

Pardini, M., Leopold, A., Raymont, V., Grafman, J., 2013. A voxel-based

lesion study on facial emotion recognition after penetrating brain injury. Soc.

Cogn. Affect. Neurosci. 8, 632–639.

Decety, J., Lamm, C., 2007. The role of the right temporoparietal junction in social

interaction: how low-level computational processes contribute to

meta-cognition. Neuroscientist 13, 580–593.

Dunbar, R.I.M., Shultz, S., 2007. Evolution in the social brain. Science 317,

1344–1347.

Eickhoff, S.B., Stephan, K.E., Mohlberg, H., Grefkes, C., Fink, G.R., Amunts, K., Zilles, K., 2005. A new SPM toolbox for combining probabilistic cytoarchitectonic maps and functional imaging data. Neuroimage 25, 1325–1335.

Eldridge, L.L., Knowlton, B.J., Furmanski, C.S., Bookheimer, S.Y., Engel, S.A., 2000. Remembering episodes: a selective role for the hippocampus during retrieval. Nat. Neurosci. 3, 49–52.

Evans, A.C., Kamber, M., Collins, D.L., MacDonald, D., 1994. An MRI-Based Probabilistic Atlas of Neuroanatomy, In: Shorvon, S.D., Fish, D.R., Andermann, F., Bydder, G.M., Stefan, H. (Eds.), Magnetic Resonance Scanning and Epilepsy. vol. 264 Springer, New York, pp. 263–274.

Friston, K.J., Jezzard, P., Turner, R., 1994a. Analysis of functional MRI time-series. Hum. Brain Mapp. 1, 153–171.

Friston, K.J., Worsley, K.J., Frackowiak, R.S., Mazziotta, J.C., Evans, A.C., 1994b. Assessing the significance of focal activations using their spatial extent. Hum Brain Mapp. 1, 210-220.

Friston, K.J., Ashburner, J., Frith, C.D., Poline, J.-B., Heather, J.D., Frackowiak, R.S.J., 1995. Spatial registration and normalization of images. Hum. Brain Mapp. 2, 165–188.

Friston, K.J., Holmes, A., Poline, J.B., Price, C.J., Frith, C.D., 1996. Detecting

activations in PET and fMRI: levels of inference and power. Neuroimage 4,

223–235.

Friston, K.J., Glaser, D.E., Henson, R.N.A., Kiebel, S., Phillips, C., Ashburner, J., 2002.

Classical and Bayesian inference in neuroimaging: applications. Neuroimage

16, 484–512.

Friston, K.J., Ashburner, J., Kiebel, S.J., Nichols., T.E., Penny, W.D., 2007. Statistical

Parametric Mapping: The Analysis of Functional Brain Images. Academic

Press, London.

Frith, U., Frith, C.D., 2003. Development and neurophysiology of mentalizing. Philos.

Trans. R. Soc. Lond. B Biol. Sci. 358, 459–473.

Frith, C.D., 2007. The social brain? Philos. Trans. R. Soc. Lond. B. Biol. Sci. 362,

671–678.

Gao, X., Maurer, D., Nishimura, M., 2013. Altered representation of facial expressions

after early visual deprivation. Front. Psychol. 4, 878.

Goel, V., Grafman, J., Sadato, N., Hallett, M., 1995. Modeling other minds.

Neuroreport 6, 1741–1746.

Haxby, J.V., Gobbini, M.I., Furey, M.L., Ishai, A., Schouten, J.L., Pietrini, P., 2001.

Distributed and overlapping representations of faces and objects in ventral

temporal cortex. Science 293, 2425–2430.

Haynes, J.D., Sakai, K., Rees, G., Gilbert, S., Frith, C., Passingham, R.E., 2007.

Reading hidden intentions in the human brain. Curr. Biol. 17, 323–328.

Hendriks, M.C., Van Boxtel, G.J., Vingerhoets, A.J.J.M., 2007. An event-related

potential study on the early processing of crying faces. Neuroreport 18,

631–634.

Holmes, A.P., Friston, K.J., 1998. Generalizability, random effects and population

inference. Neuroimage 7, S754.

Hornak, J., Rolls, E.T., Wade, D., 1996. Face and voice expression identification in

patients with emotional and behavioural changes following ventral frontal

lobe damage. Neuropsychologia 34, 247–261.

Hornak, J., Bramham, J., Rolls, E.T., Morris, R.G., O'Doherty, J., Bullock, P.R., Polkey,

C.E., 2003. Changes in emotion after circumscribed surgical lesions of the

orbitofrontal and cingulate cortices. Brain 126, 1691–1712.

Kennedy, D.P., Adolphs, R., 2012. The social brain in psychiatric and neurological

disorders. Trends. Cogn. Sci. 16, 559–572

Kitada, R., Okamoto, Y., Sasaki, A.T., Kochiyama, T., Miyahara, M., Lederman, S.J.,

Sadato, N., 2013. Early visual experience and the recognition of basic facial

expressions: involvement of the middle temporal and inferior frontal gyri

during haptic identification by the early blind. Front. Hum. Neurosci. 7, 7.

Koster-Hale, J., Saxe, R., 2013. Theory of mind: a neural prediction problem. Neuron

79, 836–848.

Kriegeskorte, N., Simmons, W.K., Bellgowan, P.S.F., Baker, C.I., 2009. Circular

analysis in systems neuroscience: the dangers of double dipping. Nat.

Neurosci. 12, 535–540.

Krueger, F., Barbey, A.K., Grafman, J., 2009. The medial prefrontal cortex mediates

social event knowledge. Trends Cogn. Sci. 13, 103–109.

Lennox, B.R., Jacob, R., Calder, A.J., Lupson, V., Bullmore, E.T., 2004. Behavioural

and neurocognitive responses to sad facial affect are attenuated in patients

with mania. Psychol. Med. 34, 795–802.

Mason, M.F., Norton, M.I., Van Horn, J.D., Wegner, D.M., Grafton, S.T., Macrae, C.N.,

2007. Wandering minds: the default network and stimulus-independent

thought. Science 315, 393–395.

Matsuda, H., 2007. Role of neuroimaging in Alzheimer's disease, with emphasis on

brain perfusion SPECT. J. Nucl. Med. 48, 1289–1300.

Meredith, M.A., Stein, B.E., 1983. Interactions among converging sensory inputs in the

superior colliculus. Science 221, 389-391.

Minoshima, S., Giordani, B., Berent, S., Frey, K.A., Foster, N.L., Kuhl, D.E., 1997.

Metabolic reduction in the posterior cingulate cortex in very early

Alzheimer's disease. Ann. Neurol. 42, 85–94.

Mitchell, J.P., 2008. Activity in right temporo-parietal junction is not selective for

theory-of-mind. Cereb. Cortex 18, 262–271.

Miyashita, Y., 2004. Cognitive memory: cellular and network machineries and their

top-down control. Science 306, 435–440.

Morris J.S., Ohman, A., Dolan, R.J., 1998. Conscious and unconscious emotional

learning in the human amygdala. Nature 393, 467–470.

Murube, J., Murube, L., Murube, A., 1999. Origin and types of emotional tearing. Eur. J.

Ophthalmol. 9, 77–84.

Oldfield, R.C., 1971. The assessment and analysis of handedness: the Edinburgh

inventory. Neuropsychologia 9, 97–113.

Ochsner, K.N., Bunge, S.A., Gross, J.J., Gabrieli, J.D.E., 2002. Rethinking feelings: an

fMRI study of the cognitive regulation of emotion. J. Cogn. Neurosci. 14,

1215–1229.

Peelen, M.V., Wiggett, A.J., Downing, P.E., 2006. Patterns of fMRI activity dissociate

overlapping functional brain areas that respond to biological motion. Neuron

49, 815–822.

Peelen, M.V., Atkinson, A.P., Vuilleumier, P., 2010. Supramodal representations of

perceived emotions in the human brain. J. Neurosci. 30, 10127–10134.

Perry, A., Shamay-Tsoory, S., 2013. Understanding Emotional and Cognitive Empathy:

A neuropsychological perspective, In: Baron-Cohen, S., Lombardo, M.,

Tager-Flusberg, H. (Eds.), Understanding Other Minds: Perspectives from

developmental social neuroscience. Oxford University Press, London, pp.

178–194.

Pessoa, L., McKenna, M., Gutierrez, E., Ungerleider, L.G., 2002. Neural processing of

emotional faces requires attention. Proc. Natl. Acad. Sci. USA. 99,

11458–11463.

Phan, K.L., Wager, T., Taylor, S.F., Liberzon, I., 2002. Functional neuroanatomy of

emotion: a meta-analysis of emotion activation studies in PET and fMRI.

Neuroimage 16, 331–348.

Provine, R.R., Krosnowski, K.A., Brocato, N.W., 2009. Tearing: Breakthrough in

human emotional signaling. Evol. Psychol. 7, 52–56.

Raij, T., Uutela, K., Hari, R., 2000. Audiovisual integration of letters in the human brain.

Neuron 28, 617–625.

Rolls, E.T., 2004. The functions of the orbitofrontal cortex. Brain Cogn. 55, 11–29.

Ranganath, C., Cohen, M.X., Dam, C., D'Esposito, M., 2004. Inferior temporal,

prefrontal, and hippocampal contributions to visual working memory

maintenance and associative memory retrieval. J. Neurosci. 24, 3917–3925.

Saxe, R., Powell, L.J., 2006. It's the thought that counts: specific brain regions for one

component of theory of mind. Psychol. Sci. 17, 692–699.

Satpute, A.B., Lieberman, M.D., 2006. Integrating automatic and controlled processes

into neurocognitive models of social cognition. Brain Res. 1079, 86–97.

Scholz, J., Triantafyllou, C., Whitfield-Gabrieli, S., Brown, E.N., Saxe, R., 2009.

Distinct regions of right temporo-parietal junction are selective for theory of

mind and exogenous attention. PLoS One 4, e4869.

Shattuck, D.W., Mirza, M., Adisetiyo, V., Hojatkashani, C., Salamon, G., Narr, K.L.,

Poldrack, R.A., Bilder, R.M., Toga, A.W., 2008. Construction of a 3D

probabilistic atlas of human cortical structures. Neuroimage 39, 1064–1080.

Skerry, A.E., Saxe, R., 2014. A common neural code for perceived and inferred emotion.

J. Neurosci. 34, 15997–16008.

Spreng, R.N., Mar, R.A., Kim, A.S.N., 2009. The common neural basis of

autobiographical memory, prospection, navigation, theory of mind, and the

default mode: a quantitative meta-analysis. J. Cogn. Neurosci. 21, 489–510.

Stanley, D. A., Adolphs, R., 2013. Toward a neural basis for social behavior. Neuron 80,

816–826

Stevenson, R.A., Kim, S., James, T.W., 2009. An additive-factors design to

disambiguate neuronal and areal convergence: measuring multisensory

interactions between audio, visual, and haptic sensory streams using fMRI.

Exp. Brain Res. 198, 183–194.

Van Overwalle, F., 2009. Social cognition and the brain: a meta-analysis. Hum. Brain

Mapp. 30, 829–858.

Van Overwalle, F., Baetens, K., 2009. Understanding others' actions and goals by

mirror and mentalizing systems: a meta-analysis. Neuroimage 48, 564–584.

Vytal, K., Hamann, S., 2010. Neuroimaging support for discrete neural correlates of

basic emotions: a voxel-based meta-analysis. J. Cogn. Neurosci. 22,

2864–2885.

Wagner, A.D., Shannon, B.J., Kahn, I., Buckner, R.L., 2005. Parietal lobe contributions

to episodic memory retrieval. Trends Cogn. Sci. 9, 445–453.

Willis, M.L., Palermo, R., Burke, D., McGrillen, K., Miller, L., 2010. Orbitofrontal

cortex lesions result in abnormal social judgments to emotional faces.

Neuropsychologia 48, 2182–2187.

Willis, M.L., Palermo, R., McGrillen, K., Miller, L., 2014. The nature of facial

expression recognition deficits following orbitofrontal cortex damage.

Neuropsychology 28, 613–623.

Winston, J.S., O'Doherty, J., Dolan, R.J., 2003. Common and distinct neural responses

during direct and incidental processing of multiple facial emotions.

Neuroimage 20, 84–97.

Worsley, K.J., Friston, K.J., 1995. Analysis of fMRI time-series revisited--again.

Neuroimage 2, 173–181.

9. Tables

Table 1. Predefined contrasts

Regressors	Sad			Neutral			Baseline (B)
	ST	SC	S	NT	NC	N	
Tears - NoTears	1	0	-1	1	0	-1	0
Circles - NoTears	0	1	-1	0	1	-1	0
Tears - Circles	1	-1	0	1	-1	0	0
Sad - Neutral expressions	1	1	1	-1	-1	-1	0
Interaction effects	1	-1	0	-1	1	0	0
	-1	1	0	1	-1	0	0

Table 2. Tears minus NoTears

Spatial extent test		MNI coordinates (mm)			t-value(37)	Location	
Cluster size (mm³)	p-values	x	y	z		Side	Area
Tears minus NoTears [(ST+NT) - (S+N)] (Figure 3)
37656	<0.001	-26	-70	60	4.63	L	Superior parietal lobule
		-24	-80	46	3.11	L	Superior occipital gyrus
		-46	-68	24	5.82	L	TPJ
		-50	-64	-2	7.36	L	Middle temporal gyrus
		-48	-60	-4	7.55	L	Inferior temporal gyrus
		-50	-68	-4	6.12	L	Middle occipital gyrus
		-42	-60	-10	5.00	L	Fusiform gyrus
		-50	-70	-10	4.60	L	Inferior occipital gyrus
		-56	-6	-14	3.68	L	Superior temporal gyrus
		-26	-6	-18	3.90	L	Amygdala[a]
		-32	-28	-20	4.68	L	Hippocampus[b]
		-6	-28	-26	4.09	L	Brainstem
17872	<0.001	-24	28	50	3.46	L	Middle frontal gyrus
		-16	38	44	4.19	L	dmPFC
		-8	20	-6	2.80	L	Caudate nucleus
		10	22	-6	3.21	R	Caudate nucleus
		-2	50	-12	6.03	L	vmPFC
		8	60	16	3.37	R	vmPFC
		0	26	-18	6.37		mOFC
17528	<0.001	20	-66	64	4.56	R	Superior parietal lobule
		28	-78	46	3.51	R	Superior occipital gyrus
		58	-66	20	4.19	R	TPJ
		50	-76	18	3.93	R	Middle occipital gyrus
		52	-56	-4	5.95	R	Middle temporal gyrus
		52	-62	-6	6.20	R	Inferior temporal gyrus
		48	-64	-10	4.21	R	Inferior occipital gyrus
		46	-50	-16	4.08	R	Fusiform gyrus
11312	<0.001	-4	-56	36	5.60	L	Precuneus
		-8	-54	26	5.33	L	Posterior cingulate gyrus
		4	-52	24	3.32	R	Posterior cingulate gyrus

The threshold size of activation was $p < 0.05$, corrected for multiple comparisons over the whole brain, when the height threshold was set at $t(37) > 2.72$. x, y, and z are stereotaxic coordinates (mm). R, right hemisphere; L, left hemisphere. dmPFC, dorsomedial prefrontal cortex; vmPFC, ventromedial prefrontal cortex; mOFC, medial orbitofrontal cortex; TPJ, temporoparietal junction. [a, b] Probability values on

cytoarchitectonic maps (Amunts et al., 2005): [a] 80% for the amygdala and 40% for the

hippocampus; [b] 50% for the hippocampus.

Table 3. Circles minus NoTears

Spatial extent test		MNI coordinates (mm)			t-value(37)	Location	
Cluster size (mm^3)	p-values	x	y	z		Side	Area
Circles minus NoTears [(SC+NC) - (S+N)] (Figure 4)							
163152	<0.001	-24	-74	50	7.91	L	Superior parietal lobule
		28	-70	46	7.69	R	Superior parietal lobule
		-28	-38	46	2.95	L	Postcentral gyrus
		-8	-52	46	4.05	L	Precuneus
		8	-74	54	4.64	R	Precuneus
		-24	-80	46	5.68	L	Superior occipital gyrus
		30	-74	42	5.34	R	Superior occipital gyrus
		-38	-44	40	4.70	L	Supramarginal gyrus
		42	-40	44	4.33	R	Supramarginal gyrus
		-40	-74	16	9.01	L	Middle occipital gyrus
		34	-74	30	5.61	R	Middle occipital gyrus
		-48	-66	10	6.68	L	TPJ
		44	-64	22	4.58	R	TPJ
		-46	-60	4	9.10	L	Middle temporal gyrus
		56	-52	-6	4.80	R	Middle temporal gyrus
		-46	-68	-12	8.18	L	Inferior occipital gyrus
		42	-66	-16	4.76	R	Inferior occipital gyrus
		-48	-56	-14	8.61	L	Inferior temporal gyrus
		56	-56	-14	6.08	R	Inferior temporal gyrus
		-46	-58	-18	8.57	L	Fusiform gyrus
		36	-32	-22	5.28	R	Fusiform gyrus
		-32	-26	-22	3.57	L	Parahippocampal gyrus
		36	-32	-16	4.46	R	Parahippocampal gyrus
		-46	-60	-24	5.94	L	Cerebellum
		42	-62	-22	3.60	R	Cerebellum
7136	<0.01	-38	-2	54	4.37	L	Precentral gyrus
		-36	12	28	4.20	L	Middle frontal gyrus
		-34	10	28	4.26	L	Inferior frontal gyrus

The threshold size of activation was p < 0.05, corrected for multiple comparisons over the whole brain, when the height threshold was set at t (37) > 2.72. x, y, and z are stereotaxic coordinates (mm). R, right hemisphere; L, left hemisphere. TPJ, temporoparietal junction.

Table 4. Sad minus Neutral expressions

Spatial extent test		MNI coordinates (mm)			t-value(37)	Location	
Cluster size (mm³)	p-values	x	y	z		Side	Area
Sad minus Neutral expressions [(ST+SC+S) - (NT+NC+N)] (Figure 5)							
167592	<0.001	-22	-22	68	3.92	L	Precentral gyrus
		40	-20	66	3.40	R	Precentral gyrus
		-22	-32	66	3.50	L	Postcentral gyrus
		40	-26	68	3.30	R	Postcentral gyrus
		-10	-18	60	3.83	L	Superior frontal gyrus
		14	-18	54	4.64	R	Superior frontal gyrus
		-20	36	42	6.20	L	dmPFC
		16	44	24	3.74	R	dmPFC
		-12	-56	32	3.87	L	Superior parietal lobule
		12	-56	24	3.68	R	Superior parietal lobule
		46	-38	24	3.65	R	Supramarginal gyrus
		-4	-52	20	4.60	L	Posterior cingulate gyrus
		6	-52	22	4.09	R	Posterior cingulate gyrus
		-4	-58	18	5.82	L	Precuneus
		4	-60	24	6.27	R	Precuneus
		-2	-66	16	3.07	L	Cuneus
		2	-68	24	3.97	R	Cuneus
		-12	20	6	5.41	L	Caudate nucleus
		4	20	4	4.80	R	Caudate nucleus
		-34	8	6	4.34	L	Insula
		34	8	8	4.91	R	Insula
		12	-44	4	3.05	R	Lingual gyrus
		-20	20	0	4.86	L	Putamen
		18	20	-4	4.01	R	Putamen
		-60	-2	0	3.29	L	Superior temporal gyrus
		48	-38	16	3.67	R	Superior temporal gyrus
		-4	-52	-4	3.36	L	Cerebellum
		-6	50	-10	5.65	L	vmPFC
		12	34	-10	5.03	R	vmPFC
		-30	-34	-10	4.94	L	Parahippocampal gyrus
		28	-20	-22	3.55	R	Parahippocampal gyrus
		-56	-6	-18	7.20	L	Middle temporal gyrus
		54	-2	-20	5.70	R	Middle temporal gyrus
		0	24	-20	5.36		mOFC
		-34	-10	-20	6.03	L	Hippocampus[a]
		32	-16	-18	4.96	R	Hippocampus[b]
		-34	-8	-20	5.32	L	Amygdala[c]
		38	-2	-22	4.87	R	Amygdala[d]
		-38	-16	-22	4.65	L	Fusiform gyrus
		40	-26	-16	3.04	R	Fusiform gyrus
		-50	-20	-22	5.08	L	Inferior temporal gyrus

The threshold size of activation was $p < 0.05$, corrected for multiple comparisons over the whole brain, when the height threshold was set at t (37) > 2.72. x, y, and z are stereotaxic coordinates (mm). R, right hemisphere; L, left hemisphere. dmPFC,

dorsomedial prefrontal cortex; vmPFC, ventromedial prefrontal cortex; mOFC, medial

orbitofrontal cortex; TPJ, temporoparietal junction. [a–d] Probability values on

cytoarchitectonic maps (Amunts et al., 2005): [a] 50% for the hippocampus and 40% for

the amygdala; [b] 90% for the hippocampus; [c] 40% for the amygdala and 30% for the

hippocampus; [d] 50% for the amygdala.

Table 5. The supra-additive effect between Tears and Sad expressions

Spatial extent test		MNI coordinates (mm)			t-value(37)	Location	
Cluster size (mm³)	p-values	x	y	z		Side	Area
Interaction [(ST-SC) - (NT-NC)] (Supra-additive effect, Figure 6)							
17864	<0.001	-8	-46	30	3.72	L	Posterior cingulate gyrus
		8	-42	34	3.05	R	Posterior cingulate gyrus
		-10	-56	22	4.01	L	Precuneus
		12	-50	10	4.51	R	Precuneus
		0	-68	20	3.56		Cuneus
		16	-40	2	4.09	R	Parahippocampal gyrus
		0	-74	0	5.00		Lingual gyrus
		0	-72	-10	2.75		Cerebellum
		20	-10	-12	3.12	R	Amygdala/Hippocampus[a]
		22	-14	-12	4.14	R	Hippocampus[b]
11440	<0.001	-4	44	22	3.21	L	dmPFC
		-10	44	4	4.45	L	vmPFC
		12	46	4	3.81	R	vmPFC
		10	36	-16	3.94	R	mOFC
4088	<0.05	-34	-30	-14	4.24	L	Parahippocampal gyrus
		-30	-10	-16	6.23	L	Amygdala[c]
		-30	-12	-16	7.16	L	Hippocampus[d]
Interaction [(NT-NC) - (ST-SC)]							
			n.s.				

The threshold size of activation was $p < 0.05$, corrected for multiple comparisons over the whole brain, when the height threshold was set at $t (37) > 2.72$. x, y, and z are stereotaxic coordinates (mm). R, right hemisphere; L, left hemisphere. dmPFC, dorsomedial prefrontal cortex; vmPFC, ventromedial prefrontal cortex; mOFC, medial orbitofrontal cortex. [a–d] Probability values on cytoarchitectonic maps (Amunts et al., 2005): [a] 40% for the amygdala and 40% for the hippocampus; [b] 50% for the hippocampus; [c] 40% for the amygdala and 30% for the hippocampus; [d] 60% for the hippocampus and 30% for the amygdala. n.s. indicates that no significant activation was found.
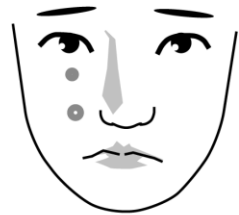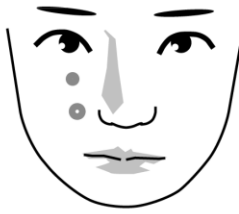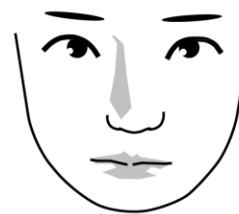
Table 6. Tears minus NoTears in a separate experiment

Spatial extent test		MNI coordinates (mm)			t-value(22)	Location	
Cluster size (mm³)	p-values	x	y	z		Side	Area
Tears minus NoTears [(ST+NT) - (S+N)] in a separate experiment (Figure 7)							
20872	<0.001	-40	-64	18	6.38	L	TPJ*
		-46	-74	18	6.27	L	Middle occipital gyrus
		-56	-70	6	5.12	L	Middle temporal gyrus
		-48	-68	-8	4.51	L	Inferior temporal gyrus
		-48	-72	-10	4.86	L	Inferior occipital gyrus
		-34	-54	-16	4.39	L	Fusiform gyrus
12680	<0.001	48	-58	26	3.09	R	TPJ*
		50	-78	8	5.54	R	Middle occipital gyrus
		56	-58	2	5.07	R	Middle temporal gyrus
		50	-60	-8	4.99	R	Inferior temporal gyrus
		40	-62	-10	3.57	R	Fusiform gyrus
		48	-64	-10	4.54	R	Inferior occipital gyrus
5272	<0.01	8	22	0	2.85	R	Caudate nucleus
		-4	26	-10	3.48	L	vmPFC
		4	28	-6	3.94	R	vmPFC
		-2	42	-20	3.05	L	mOFC
		4	42	-20	5.54	R	mOFC*
4992	<0.01	28	-44	62	3.21	R	Superior parietal lobule
		28	-28	58	4.25	R	Postcentral gyrus
		32	-24	56	3.86	R	Precentral gyrus
4792	<0.01	-10	54	24	3.80	L	dmPFC
		6	52	28	3.77	R	dmPFC
		-10	60	14	4.10	L	vmPFC*
		4	58	18	3.23	R	vmPFC
3352	<0.05	-12	-54	26	4.43	L	Precuneus*
		-10	-54	24	4.25	L	Posterior cingulate gyrus

The activation was thresholded at $p < 0.05$, corrected for multiple comparisons, with the height threshold set at $t(22) > 2.82$ (corresponding to an uncorrected $p < 0.005$). x, y, and z represent the stereotaxic coordinates (mm). R, right hemisphere; L, left hemisphere. dmPFC, dorsomedial prefrontal cortex; vmPFC, ventromedial prefrontal cortex; mOFC, medial orbitofrontal cortex; TPJ, temporoparietal junction. * indicates top peak coordinates in each ROI.

A. Task design

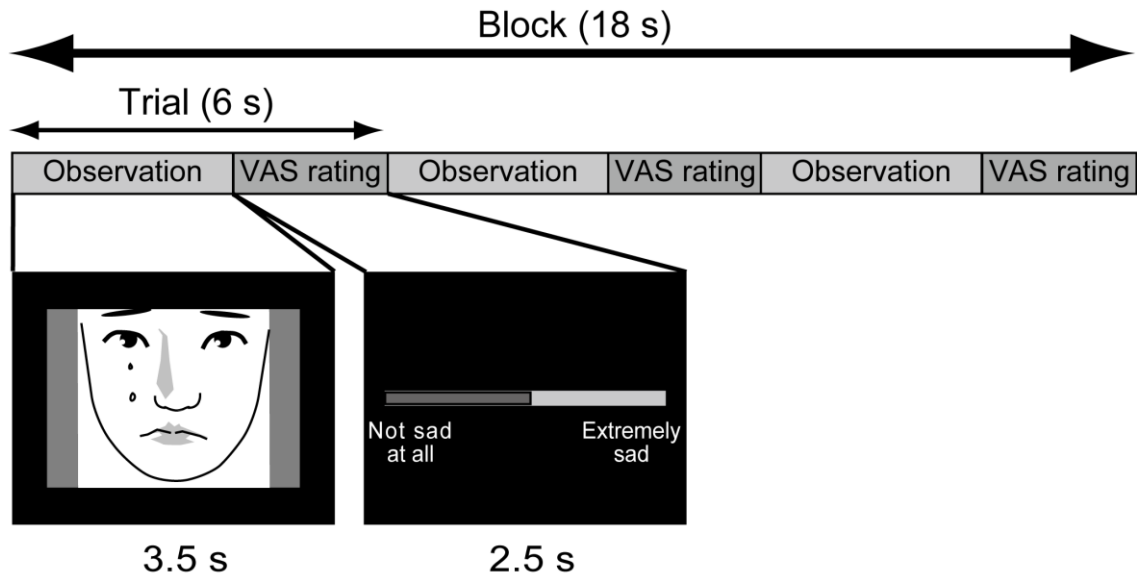|		Tears		
		With Tear (**Tears**)	With Circle (**Circles**)	Without Tear (**NoTears**)
Facial Expressions	Sadness	Sad + Tears (ST)	Sad + Circles (SC)	Sad (S)
	Neutral	Neutral + Tears (NT)	Neutral + Circles (NC)	Neutral (N)

B. Task schedule (block design)

Block (18 s)

Trial (6 s)

| Observation | VAS rating | Observation | VAS rating | Observation | VAS rating |

Not sad at all — Extremely sad

3.5 s   2.5 s

Figure 1. Experimental design

(A) Task designs.

I adopted a within-subjects factorial design with two factors: Tears and Facial

expressions. I extended the task design of Provine et al. (2009) by including two levels

of Facial Expressions (Sad and Neutral) and three levels of Tears (Tears, Circles, and

NoTears). Note that due to copyright issues these are schematics rather than the actual

stimuli.

(B) Task schedule.

I used conventional block designs in which three trials of the same condition (with

different pictures) were repeated three times in a block (18 s). The order of conditions

was pseudo-randomized. In each trial (6 s), the subject viewed the face picture for 3.5 s

and evaluated the extent of sadness of the person for 2.5 s.
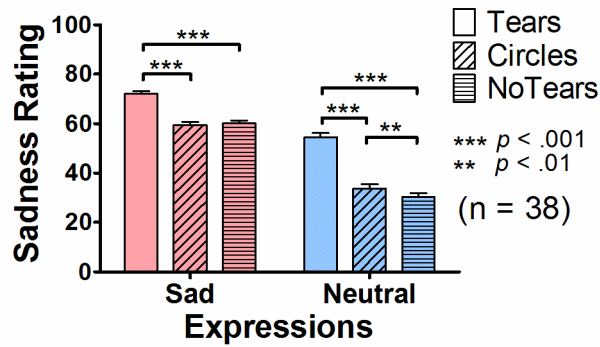
Figure 2. Behavioral results

VAS ratings of sadness perceived by the subjects. Data are presented as the mean ±

standard error of the mean (SEM). Asterisks indicate significant differences revealed by

post-hoc pairwise comparisons (with the Bonferroni correction).
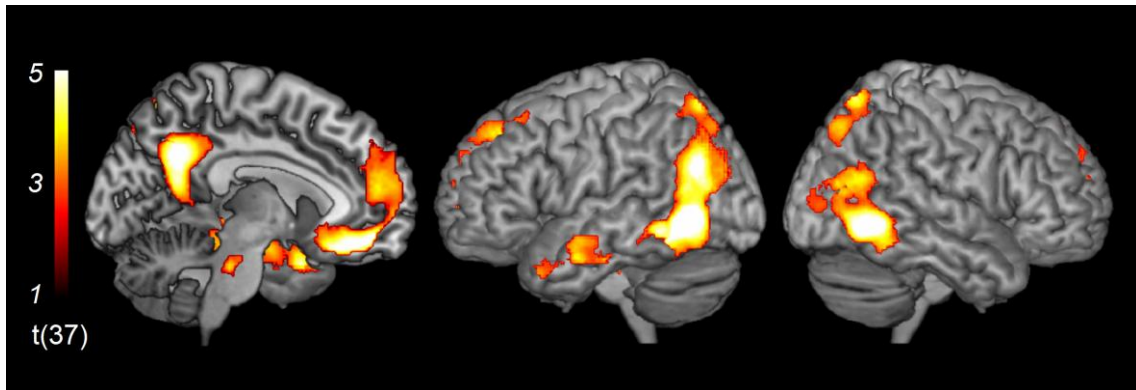
Figure 3. Tears minus NoTears

The brain activation revealed by the tear effect, via the contrast of Tears minus NoTears

[(ST + NT) - (S + N)]. The activation was thresholded at p < 0.05, corrected for

multiple comparisons over the whole brain, with the height threshold set at t (37) > 2.72

(corresponding to an uncorrected p < 0.005). The activation patterns were superimposed

on surface-rendered high-resolution MRIs unrelated to the subjects of the present study.
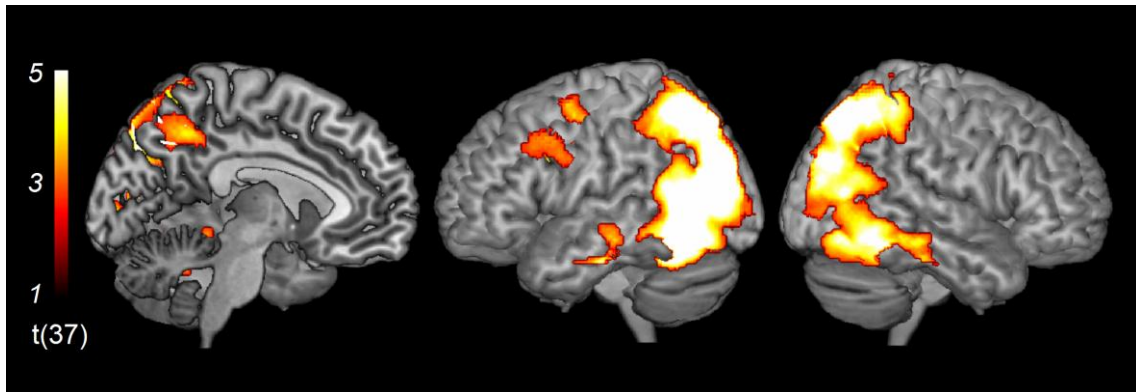
Figure 4. Circles minus NoTears

The brain activation revealed by Circles, via the contrast of Circles minus NoTears [(SC + NC) − (S + N)]. The activation was thresholded at $p < 0.05$, corrected for multiple comparisons over the whole brain, with the height threshold set at $t(37) > 2.72$ (corresponding to an uncorrected $p < 0.005$).
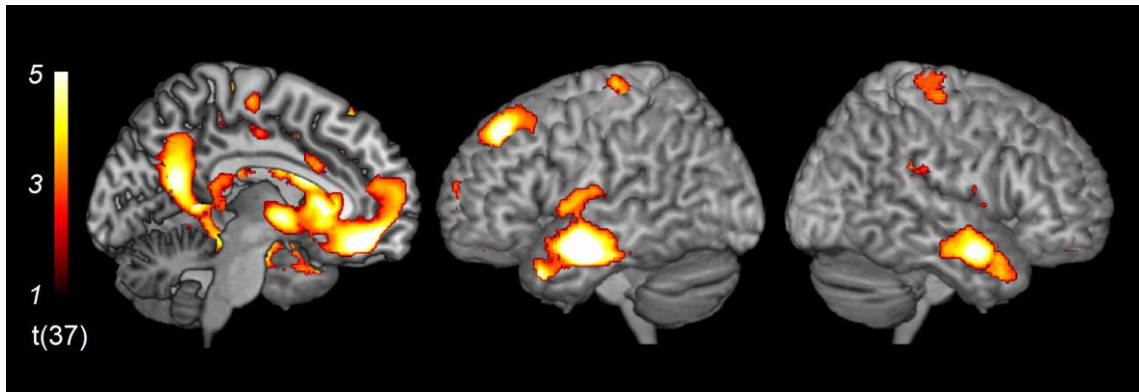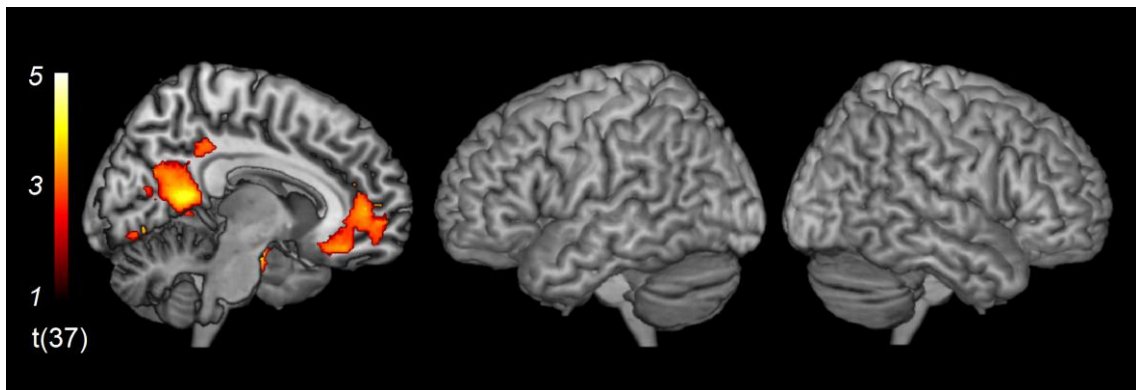
Figure 5. Sad minus Neutral expressions

The brain activation revealed by sad expressions, via the contrast of sad minus neutral

expressions [(ST + SC + S) − (NT + NC + N)]. The activation was thresholded at $p <$

0.05, corrected for multiple comparisons over the whole brain, with the height threshold

set at t (37) > 2.72 (corresponding to an uncorrected $p < 0.005$).

Figure 6. The supra-additive effect between Tears and Sad expressions

The brain activation revealed by evaluating the interaction $[(ST - SC) - (NT - NC)]$ is shown. The activation was thresholded at $p < 0.05$, corrected for multiple comparisons over the whole brain, with the height threshold set at $t(37) > 2.72$ (corresponding to uncorrected $p < 0.005$).
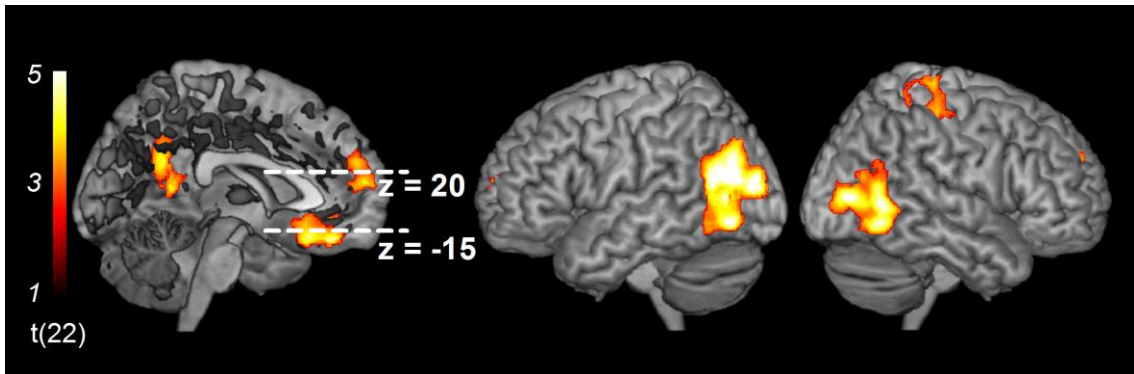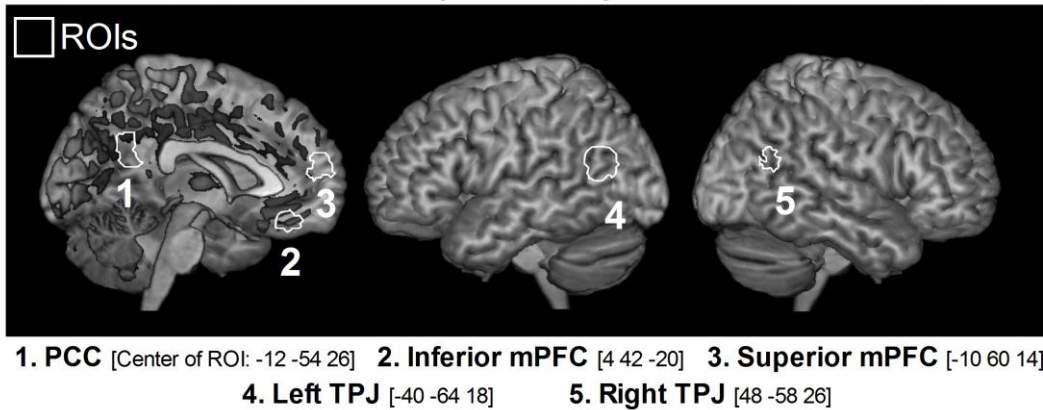
Figure 7. Tears minus NoTears in a separate experiment

In order to specify the ROIs, I depicted brain activation by evaluating the contrast of

faces with tears minus faces without tears [(ST + NT) − (S + N)] in a separate

experiment. The size of the activation was thresholded at $p < 0.05$, corrected for

multiple comparisons over the whole brain, with the height threshold set at $t(22) > 2.82$

(corresponding to an uncorrected $p < 0.005$). The dotted line at $z = 20$ represents the

border between the dmPFC and vmPFC; the dotted line at $z = −15$ shows the border

between the vmPFC and mOFC (Van Overwalle, 2009).

A: ROI definition (functionally localized by a separate experiment)

1. PCC [Center of ROI: -12 -54 26] **2. Inferior mPFC** [4 42 -20] **3. Superior mPFC** [-10 60 14]
4. Left TPJ [-40 -64 18]   **5. Right TPJ** [48 -58 26]
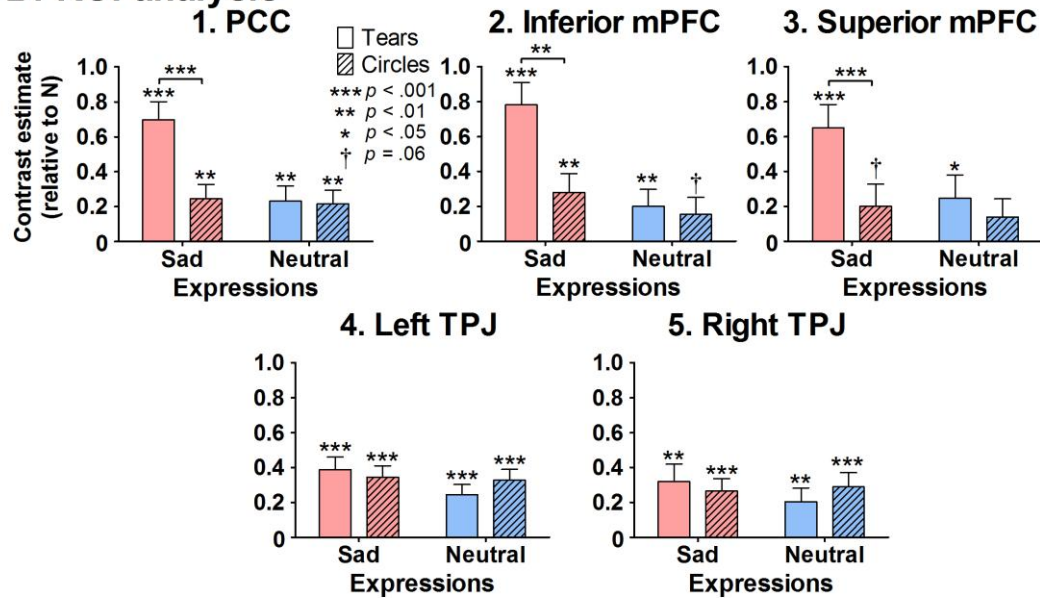
B: ROI analysis

Figure 8. ROI analysis

(A) ROI definition.

ROIs are indicated by the white lines. These regions were defined by comparing Tears

minus NoTears [(ST + SC) − (NT + N)] in a separate experiment (see **Figure 7 and**

Table 6 for more information).

(B) ROI analysis.

I averaged the contrast estimates of all voxels in each ROI and examined their patterns across the four conditions of interest (ST, SC, NT, and NC). Data are presented as the mean ± SEM. Asterisks above each bar indicate the results of one-tailed one-sample t tests on the contrast estimate (relative to the N condition). Asterisks between bars indicate the statistical significance of the post-hoc pairwise comparisons (with the Bonferroni correction). Two-way ANOVAs on these contrast estimates showed significant interactions (the supra-additive effect) in the PCC and inferior mPFC (p values < 0.05). The interaction term in the superior mPFC showed a trend toward significance ($p = 0.06$).
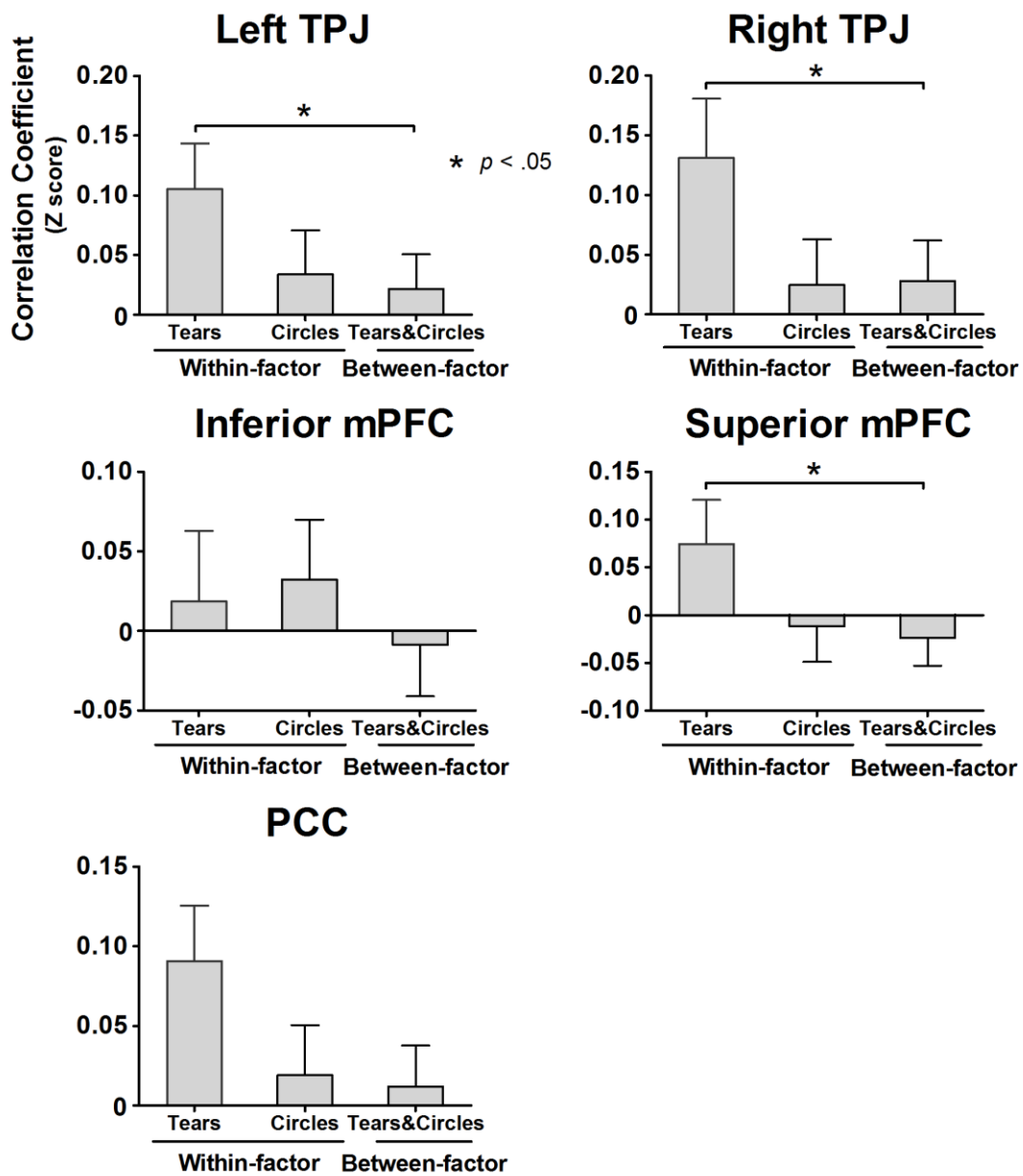
Figure 9. Multi-voxel pattern analysis (MVPA)

I conducted voxel-wise correlation analyses for each ROI. Data are presented as the

mean ± SEM. Asterisks between the conditions indicate the results of post-hoc

pair-wise comparisons (with the Bonferroni correction).